Radiol Phys Technol (2008) 1:214–222
DOI 10.1007/s12194-008-0031-4

Automated segmentation of hepatic vessels in non-contrast X-ray CT images

Suguru Kawajiri · Xiangrong Zhou · Xuejun Zhang · Takeshi Hara · Hiroshi Fujita · Ryujiro Yokoyama · Hiroshi Kondo · Masayuki Kanematsu · Hiroaki Hoshi

Received: 7 January 2008 / Revised: 29 May 2008 / Accepted: 30 May 2008 / Published online: 1 July 2008

Abstract Hepatic-vessel trees are the key structures in the liver. Knowledge of the hepatic-vessel tree is required because it provides information for liver lesion detection in the computer-aided diagnosis (CAD) system. However, hepatic vessels cannot easily be distinguished from other liver tissues in plain CT images. Automated segmentation of hepatic vessels in plain (non-contrast) CT images is a challenging issue. In this paper, an approach to automatic segmentation of hepatic vessels is proposed. The approach consists of two processing steps: enhancement of hepatic vessels and hepatic-vessel extractions. Enhancement of the vessels was performed with two techniques: (1) histogram transformation based on a Gaussian function; (2) multi-scale line filtering based on eigenvalues of a Hessian matrix. After the enhancement of the vessels, candidates of hepatic vessels were extracted by a thresholding method. Small connected regions in the final results were considered as false positives and were removed. This approach was applied to 2 normal-liver cases for whom plain CT images were obtained. Hepatic vessels segmented from the contrast-enhanced CT images of the same patient were used as the ground truth in evaluation of the performance of the proposed approach. The index of separation ratio between the CT number distributions in hepatic vessels and other liver tissue regions was also used in the evaluation. A subjective evaluation of the hepatic-vessel extraction results based on the additional 16 plain CT cases was carried out for a further validation by a radiologist. The preliminary experimental results showed that the proposed method could enhance and segment the hepatic-vessel regions even in plain CT images.

Keywords Plain X-ray CT images · Liver · Hepatic vessels · Segmentation · Image processing

S. Kawajiri (✉) · X. Zhou · T. Hara · H. Fujita
Department of Intelligent Image Information,
Division of Regeneration and Advanced Medical Sciences,
Graduate School of Medicine, Gifu University,
1-1 Yanagido, Gifu 501-1194, Japan
e-mail: kawajiri@fjt.info.gifu-u.ac.jp

X. Zhang
College of Computer Science and Information Engineering,
Guangxi University, Guangxi 530004,
People's Republic of China

R. Yokoyama
Department of Radiology Service, Gifu University Hospital,
1-1 Yanagido, Gifu 501-1194, Japan

H. Kondo · H. Hoshi
Department of Radiology, Division of Tumor Control,
Graduate School of Medicine, Gifu University,
1-1 Yanagido, Gifu 501-1194, Japan

M. Kanematsu
Department of Radiology, Gifu University Hospital,
1-1 Yanagido, Gifu 501-1194, Japan

1 Introduction

The modern multi-slice CT scanners generate a large number (500–1,000) of slices for construction of a volumetric CT image covering a large portion of the human body in 10–20 s. Although such a volumetric CT image can provide detailed information on human internal organs, the interpretations (viewing of many slices of CT images manually by use of films or a monitor for each patient case) require a great deal of time and energy. Therefore, a computer-aided diagnosis or detection (CAD) system that can support multi-lesion interpretation for multiple organs in a volumetric CT image is desirable [1]. Such a CAD

system is expected to increase the lesion(s)-detection accuracy of radiologists, and to decrease the interpretation burden and the inter- and intra-variations of diagnostic accuracy as well.

Many studies have been reported in recent research on CAD [2], for example, on the breast [3, 4], chest [5, 6], and colon [7, 8]. The liver is also one of the most diagnostically important target organs of CAD systems. Especially for the diagnosis of hepatocellular carcinoma (HCC, a primary malignancy of the liver), the liver region and the hepatic vessels in CT images provide important information for lesion detection. Therefore, automated segmentation of the liver region and recognition of hepatic vessels are required as an initial task for a liver CAD system.

Some research has been reported on the detection of liver lesion [9–12], on liver segmentation [1, 13, 14], and on hepatic-vessel visualization [15, 16], all of which was based on contrast-enhanced or multi-phase abdominal CT images. However, none of the studies focused on liver segmentation and vessel recognition in plain CT images that are used as the standard for comparison with contrast-enhanced CT images during the diagnosis of HCC. On the other hand, our research group proposed an automated approach for liver region segmentation in plain CT images by use of a probabilistic atlas, and we confirmed the efficiency and accuracy of the method as established in a large database [17]. However, hepatic-vessel segmentation and analysis based on plain CT images are still challenging and unsolved problems in the development of a liver CAD system.

In this paper, we propose a fully automated approach that is improved from our initial approach [18] to extracting the hepatic vessels including the portal vein and hepatic vein in plain CT images in preparation for hepatic-vessel-tree analysis. Density (CT number) enhancement and Hessian-based line filtering are two principal processes in the present study. In the following sections, we first describe the outline of hepatic-vessel extraction and show the details of the proposed approach in Sect. 2. Experimental results and a discussion are presented in Sects. 3 and 4, respectively. Finally, a conclusion is given in Sect. 5.

2 Methods

Although the density of hepatic-vessel regions is similar to that of the other liver tissues in plain CT images, there is a very small difference between the mean CT number of hepatic-vessel regions and the other liver tissue regions in the normal liver. Amplifying the difference in CT number between the hepatic-vessel regions and the other liver tissue regions is the main part of this approach. We propose, first, an approach to estimating the density distribution of vessel regions, and then use a Gaussian function for rough enhancement of the density distribution of the vessel regions. Finally, multi-scale line filtering based on a Hessian matrix [14, 15] is applied for precisely distinguishing the vessel regions from the other liver tissues. After the enhancement of the vessel density, a gray-level thresholding process is used for segmenting hepatic-vessel regions, and connected-component labeling is used for refining the extracted result. Figure 1 illustrates the processing flow of the proposed method, which is described in detail below.

2.1 Preprocessing

The liver tissue region is extracted automatically from the CT images by a method proposed by our research group [17]. The segmented liver region is used for limiting the spatial range for searching the hepatic-vessel locations.

Smoothing is commonly used for noise reduction before the other image-processing steps. In this study, Gaussian filter and a median filter were chosen and tested respectively in the preprocessing step to make the vessel segmentation easier.

2.2 Estimating the density distribution of hepatic-vessel regions

Liver tissues were segmented as described in Sect. 2.1. Some thick parts of the hepatic vessels appeared as “holes” surrounded by the segmented liver tissues. We extract these

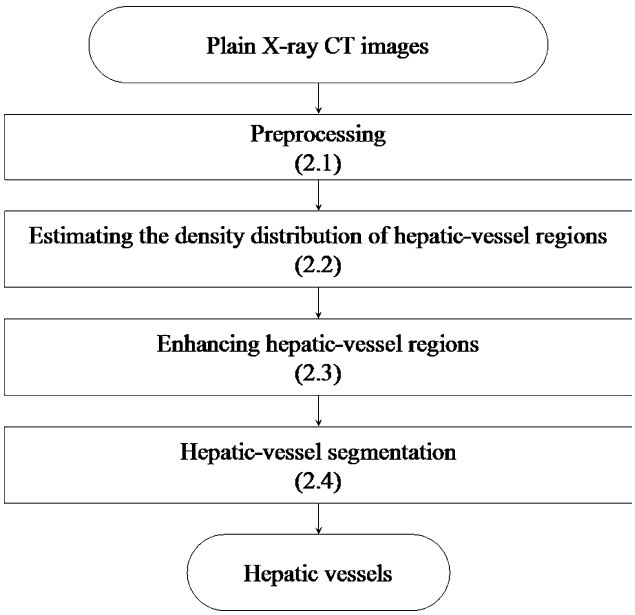

Fig. 1 Processing flow of hepatic-vessel segmentation from plain CT images

holes existing inside the segmented liver tissues by using a binary morphologic filter and regard the extracted regions as initial vessel regions. The histogram of the CT number in the initial vessel regions is regarded as the approximate density distribution of the hepatic vessels. The liver tissues and initial vessel regions are combined as a mask region that acts as a range to indicate the existence of hepatic vessels in CT images. The region outside the mask image is disregarded during the hepatic-vessel segmentation process that is described in the following sections.

2.3 Enhancing hepatic-vessel regions

The enhancement of the hepatic-vessel regions consists of two processing steps.

The first step is a histogram transformation process that generates a likelihood image of the hepatic vessels based on the estimated density distribution in the previous step. Although the hepatic-vessel regions in CT images could be enhanced in this step, some liver tissues that have a CT number similar to that of the vessel region are also enhanced and regarded as the vessel regions in the likelihood images (result of the first step).

Due to the fact that the vessel regions always appear as having a cylinder shape compared to the other false positives (FPs) that appear as having an irregular shape in the likelihood image, we use a Hessian-matrix-based line filter as the second step to reduce the FP parts of the hepatic vessels in the likelihood images. The detail of each processing step is described in the following sections.

2.3.1 Enhancement using histogram transformation

The mean value μ and standard deviation σ of the hepatic-vessel regions in CT images are estimated from the density histogram of the initial vessel regions extracted as described in Sect. 2.2. The maximum value of the histogram is used as the mean value μ, and the standard deviation σ is calculated based on the half width at half maximum of the histogram.

We define $I(\mathbf{x})$ as an original gray image; I represents the gray level, and $\mathbf{x}$ is a vector that shows the spatial position in CT images. The likelihood image of the hepatic vessels $L(\mathbf{x})$ is calculated from the following equation:

$$L(\mathbf{x}) = C \exp\left\{-\frac{(I(\mathbf{x}) - \mu)^2}{2\sigma^2}\right\}, \tag{1}$$

where C is a non-zero constant that is used for normalizing the value $L(\mathbf{x})$ within the range from 0 to C (=μ).

Equation (1) could be considered as representing a soft thresholding process. Comparing the traditional thresholding process that transfers all of the CT numbers to 0 or 1, the soft thresholding process transfers the CT number in each voxel of the CT image into a likelihood value from 0 to 1 under the condition that the density distribution of the target region can be represented by a Gaussian distribution and the parameters of the Gaussian function are known [17].

In the likelihood image, the hepatic-vessel regions appear as cylinder-shaped regions with higher density and connected together; the major part of the other regions in CT images appears as a lower-density region that is close to background and has a density of 0. Due to the overlap between the density distributions of the hepatic-vessel regions and other liver tissue regions, a part of the liver tissue regions that had a CT number similar to that of the vessels also has a high output value as calculated from Eq. (1). In order to distinguish such liver tissue regions from the hepatic-vessel regions in likelihood images, we introduced shape features for a further classification that is described in the next section.

2.3.2 Enhancement using multi-scale line filtering based on a Hessian matrix

The hepatic-vessel regions appear in the likelihood images as a set of cylinder patterns with different radii and connected together. A line filter is used for selecting the cylinder pattern in the likelihood images based on the eigenvalues of the Hessian matrix by the following equation [16]:

$$S_{\text{line}}(\mathbf{x};\sigma) = \begin{cases} |\lambda_3|\psi(\lambda_2;\lambda_3)\omega(\lambda_1;\lambda_2), & \lambda_3 \le \lambda_2 < 0, \\ 0, & \text{otherwise}, \end{cases} \tag{2}$$

where λ_1, λ_2, and λ_3 ($\lambda_1 \ge \lambda_2 \ge \lambda_3$) are eigenvalues of $\nabla^2(G(\mathbf{x}, \sigma)*L(\mathbf{x}))$ and

$$\psi(\lambda_s;\lambda_t) = \begin{cases} \left(\frac{\lambda_s}{\lambda_t}\right)^{\gamma_\psi}, & \lambda_t \le \lambda_s < 0, \\ 0, & \text{otherwise}, \end{cases} \tag{3}$$

$$\omega(\lambda_s;\lambda_t) = \begin{cases} \left(1 + \frac{\lambda_s}{|\lambda_t|}\right)^{\gamma_\omega}, & \lambda_t \le \lambda_s \le 0, \\ \left(1 - \alpha\frac{\lambda_s}{|\lambda_t|}\right)^{\gamma_\omega}, & \frac{|\lambda_t|}{\alpha} > \lambda_s > 0, \\ 0, & \text{otherwise}, \end{cases} \tag{4}$$

where $\gamma_\psi \ge 0$, $\gamma_\omega \ge 0$ and $0 < \alpha \le 1.0$.

The response of the line filter $S_{\text{line}}(\mathbf{x};\sigma)$ shows similarity to a cylinder component that has a Gaussian shape profile in the density distribution with a standard deviation σ.

In order to adapt to the enhancement of the hepatic vessels that have different diameters, the line filter $S_{\text{line}}(\mathbf{x};\sigma)$ is expanded to a multi-scale format by the following equation:

$$M(\mathbf{x}) = \max_{\sigma_i} \sigma_i^2 S_{\text{line}}(\mathbf{x};\sigma_i), \tag{5}$$

where σ_i corresponds to the diameter of the target vessels and is calculated with the following equation:

$$\sigma_i = s^{i-1}\sigma_0, \tag{6}$$

where s and i are constant values determined experimentally.

2.4 Hepatic-vessel segmentation

A combination of gray-level thresholding, connected-component labeling, and isolated small 3-D region deleting is used for hepatic-vessel segmentation. These processes are utilized for identifying the hepatic-vessel regions in the likelihood images generated as described in Sect. 2.3. Gray-level thresholding is used for making alternate selections of hepatic-vessel regions from the other regions. Connected-component labeling and deleting procedures are used for refining the vessel extraction result. Isolated 3-D regions with a small volume are deleted as the FPs that may be other components in a liver or may be image noise in the likelihood image. The threshold value th_g of the gray-level thresholding was determined by a p-tile method ($p = 50[\%]$) automatically, and th_v of the connected-component processing (labeling and deleting) was set to 100 based on our experience. In our initial approach [18], th_g and th_v were constant.

3 Experiments

The proposed approach was applied to two patient cases of X-ray CT images of the torso. Each CT case was scanned by a multislice CT scanner (UltraSpeed of Yokogawa GE Healthcare, Tokyo, Japan) with a common protocol (120 kV/Auto mA) and covered the whole human torso with about 1,000 slices, an isotopic spatial resolution of about 0.6 mm, and a density (CT number) resolution of 12 bits. Contrast-enhanced CT images for each patient were also scanned and used as gold standard for evaluation of hepatic-vessel extraction results. The gold standard in each CT case was decided by tracing of hepatic vessels in

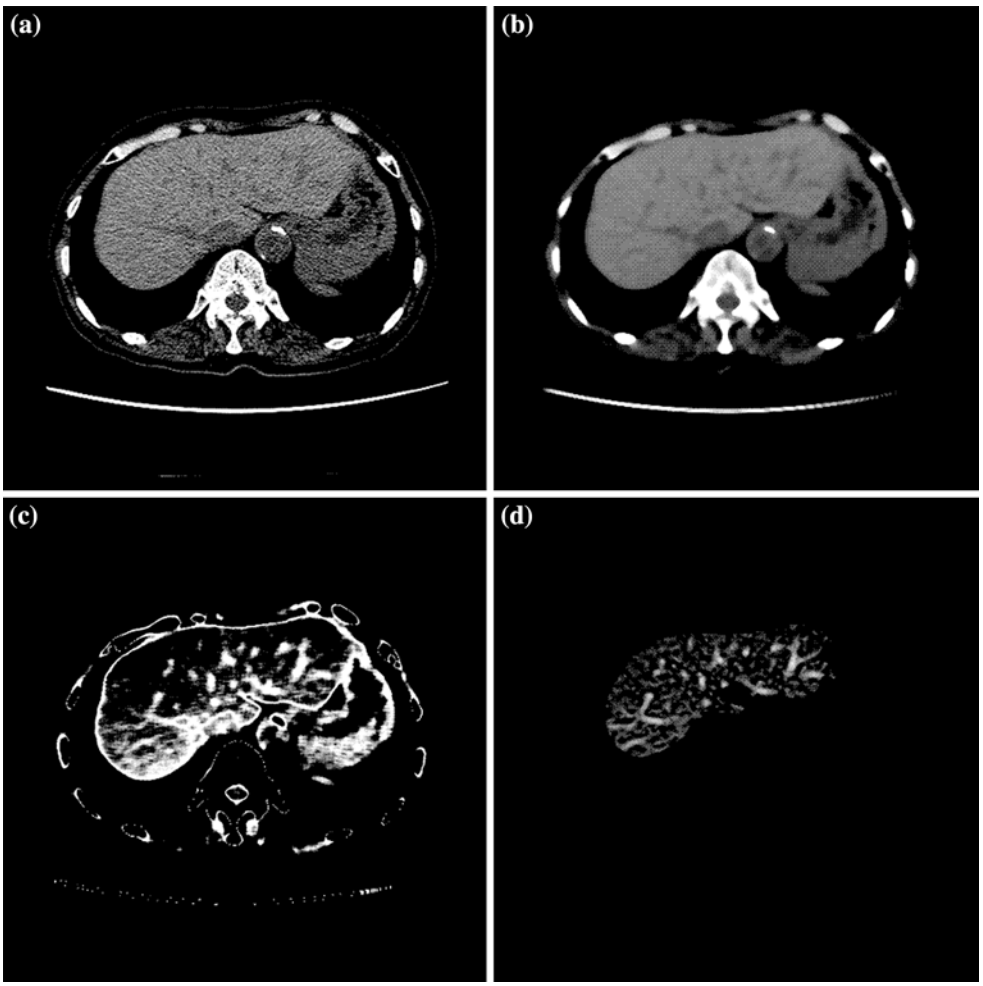

Fig. 2 Results of the hepatic-vessel segmentation approach. **a** CT image (1 axial slice). **b** Result of the density-enhancing process by use of a Gaussian function. **c** Likelihood image: result of use of median filter (mask size: 7 × 7 × 7). **d** Result of use of the multi-scale line filter based on eigenvalues of Hessian matrix

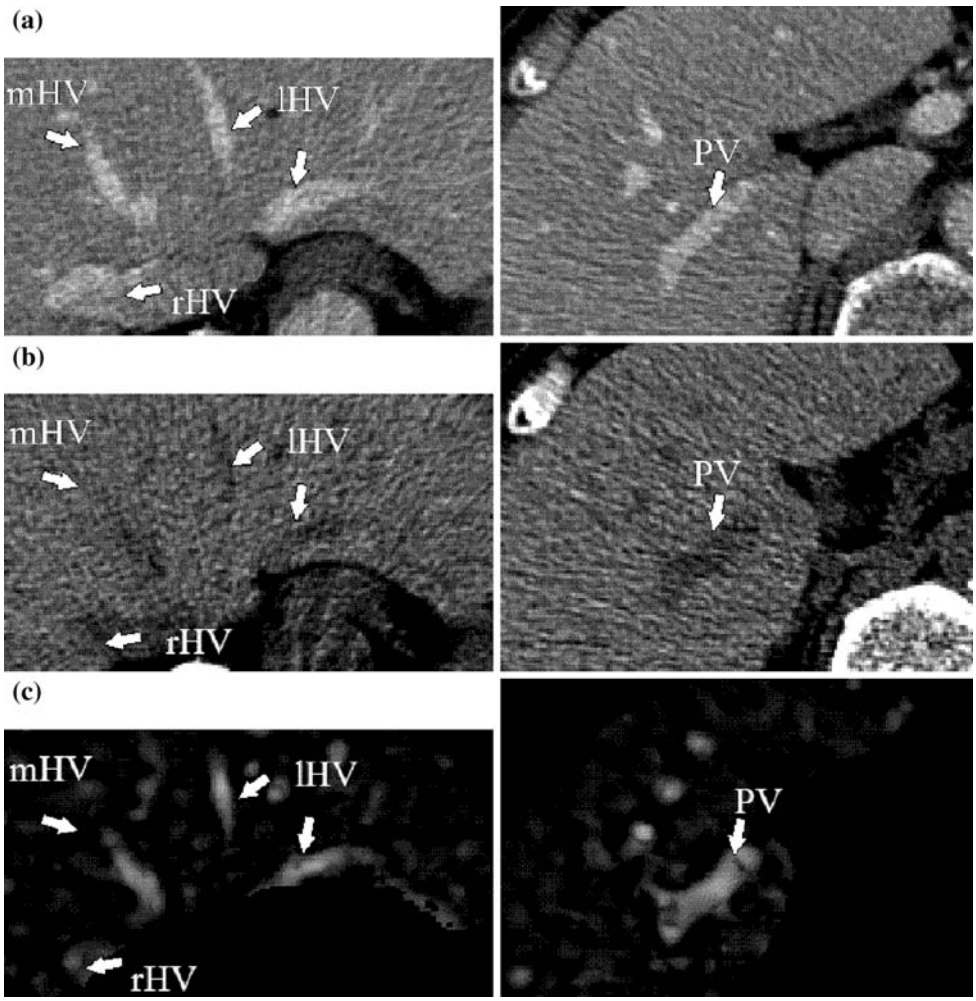

Fig. 3 Comparing the result of hepatic vessel enhancement with contrast-enhanced CT images of the same patient. **a** Two slices of contrast-enhanced CT images. **b** Two slices of plain CT images. **c** Results after enhancement processing in non-contrast CT images. *rHV* right hepatic vein, *mHV* middle hepatic vein, *lHV* left hepatic vein, *PV* portal vein

plain CT images manually by comparing the contrast-enhanced CT image of the same patient. The decision on the gold standard was inspected by a radiologist specialized in liver diagnosis. The parameters in Eqs. (2)–(6) were set as $s = 1.5$, $\sigma_0 = 1.5$, $i = 1, 2, 3$, $\alpha = 0.25$, and $\gamma_\psi = \gamma_\omega = 0.5$, which were designed to enhance hepatic vessels with diameters of more than 3 mm in the CT images.

4 Results and discussion

Figure 2 shows the effects of each processing step of our approach (Fig. 1). The hepatic vessels in the original CT images (Fig. 2a) appear as dark line patterns surrounded by image noise. After preprocessing, the image noise was suppressed, and the main parts of the hepatic vessels could be observed in the CT images. However, the difference between the CT number of vessels and that of liver tissues was very small, and the hepatic-vessel regions were not very clear for observation (Fig. 2b). Figure 2c shows the effect of enhancement by use of the Gaussian distribution. The result (likelihood image) shows that the regions that have CT numbers similar to that of the hepatic vessels were selected and appeared as the high-density regions in the resulting images. However, many FP regions appeared with the hepatic-vessel regions, and the distinction of the hepatic vessels from the other tissues by use of contrast was still difficult. After the processing of multi-scale line filtering by use of the eigenvalues of the Hessian matrix, the hepatic-vessel regions were selected and separated correctly from the other tissue regions in the CT images (Fig. 2d). Therefore, the observation of the hepatic vessels became clearer and easier.

Compared with the contrast-enhanced X-ray CT images of the same patient, we confirmed that the main parts of the hepatic vessels (lHV: left hepatic vein, mHV: middle hepatic vein, rHV: right hepatic vein, and PV: portal vein) in the plain CT images were correctly enhanced and selected, as shown in Fig. 3. This result shows the potential for the visualization of the main parts of the hepatic vessels in plain CT images and the usefulness of our proposed method.

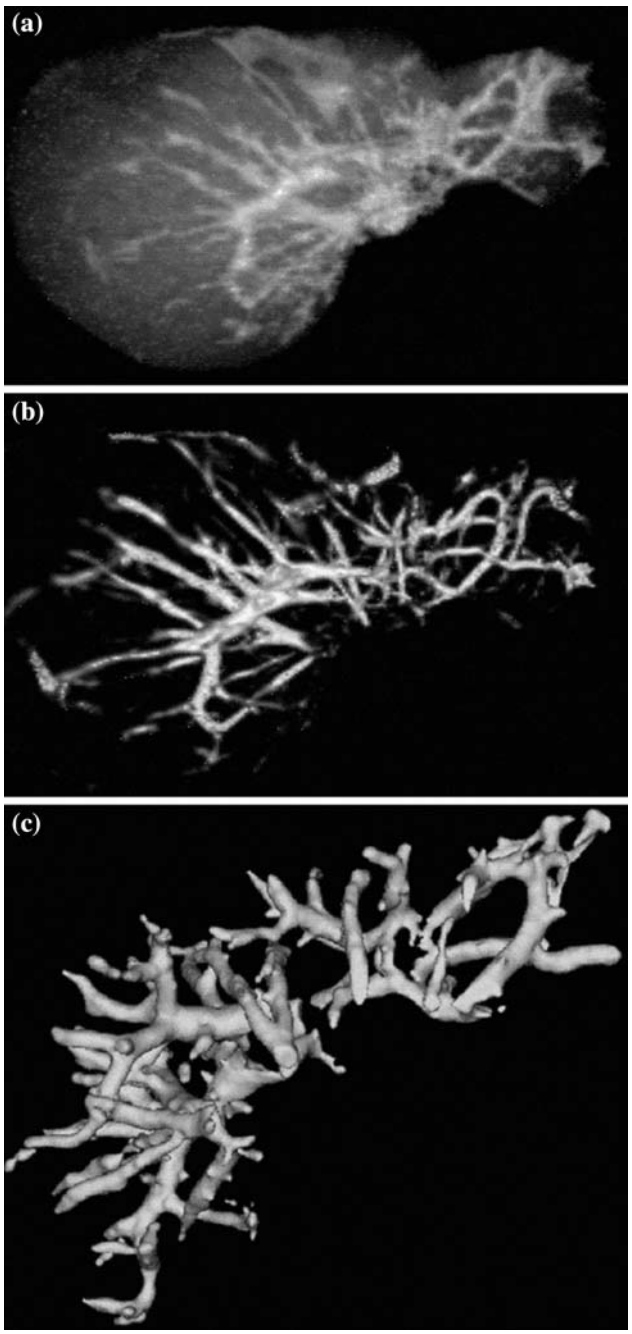

Fig. 4 3-D view of the liver and hepatic-vessel tree. **a** Volume rendering of contrast-enhanced CT images. **b** Volume rendering of the hepatic vessels after the enhancement process. **c** Surface rendering of the segmentation result for hepatic vessels

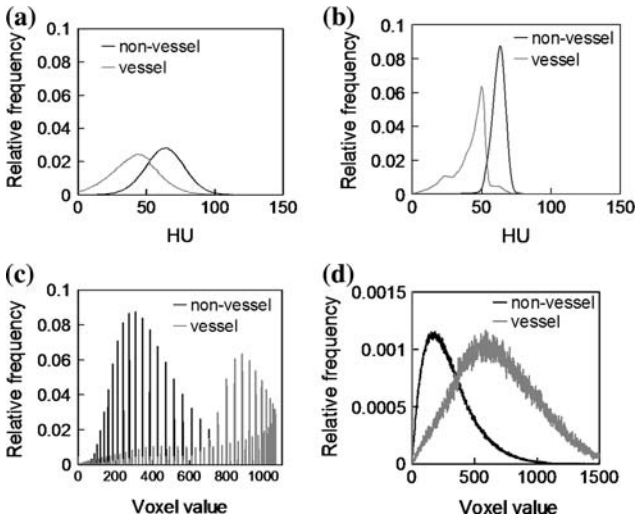

Fig. 5 Histograms of liver vessel and non-vessel regions in each processing step from **a** original CT images, **b** result of use of Gaussian filter, **c** result of contrast enhancement by use of a Gaussian function, and **d** result of use of the multi-scale line filter

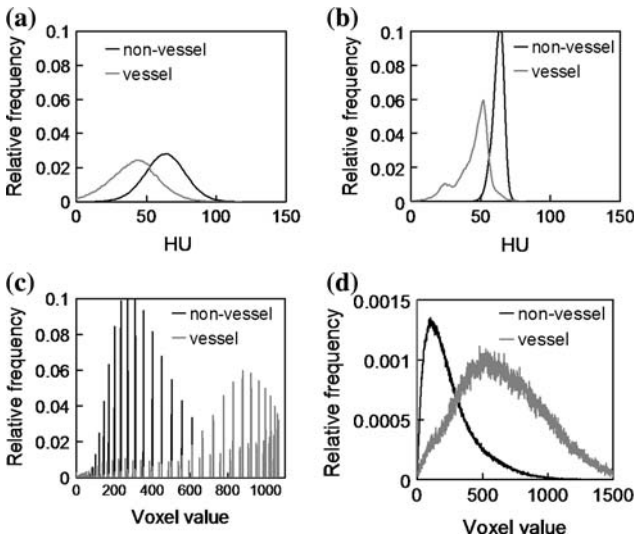

Fig. 6 Histograms of liver vessel and non-vessel regions in each processing step from **a** original CT images, **b** result of use of median filter, **c** result of contrast enhancement by use of a Gaussian function, and **d** result of use of the multi-scale line filter

Volume rendering and surface rendering are two conventional methods for the visualization of CT images in clinical medicine. However, observing the hepatic-vessel structures in 3-D by use of plain CT images is impossible. After the enhancement by use of the proposed method, we confirmed that the hepatic-vessel trees can be visualized in 3-D by volume rendering or surface rendering, as shown in Fig. 4. The proposed approach provides the possibility to view the 3-D hepatic-tree structures in the plain CT images that are widely used for screening purposes.

Two kinds of algorithms are used for noise smoothing. The experimental results showed that a median filter (mask size: $7 \times 7 \times 7$ voxels) was the most effective for noise reduction in this study. However, the computation cost for median filter is very high (applying a median filter by using a mask size of $7 \times 7 \times 7$ voxels to a CT image (size: $512 \times 512 \times 512$) requires about 3 hours with use of a CPU AMD Opteron 2.4 GHz). On the other hand, the

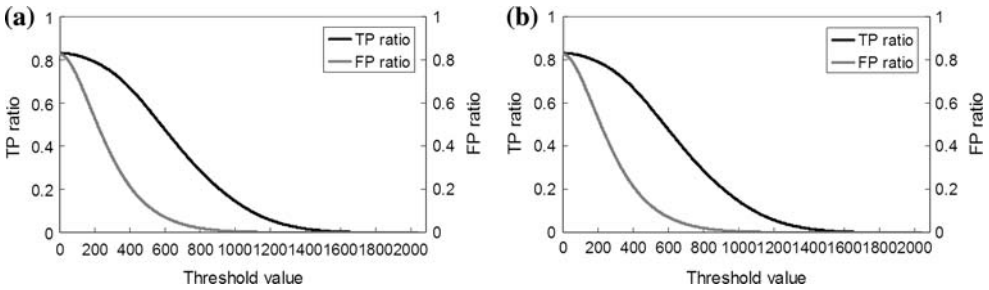

Fig. 7 Two curves between TP ratio (extraction ratio) or FP ratio (over-extraction ratio) and threshold values of hepatic-vessel region(s) for two cases, *a* and *b*

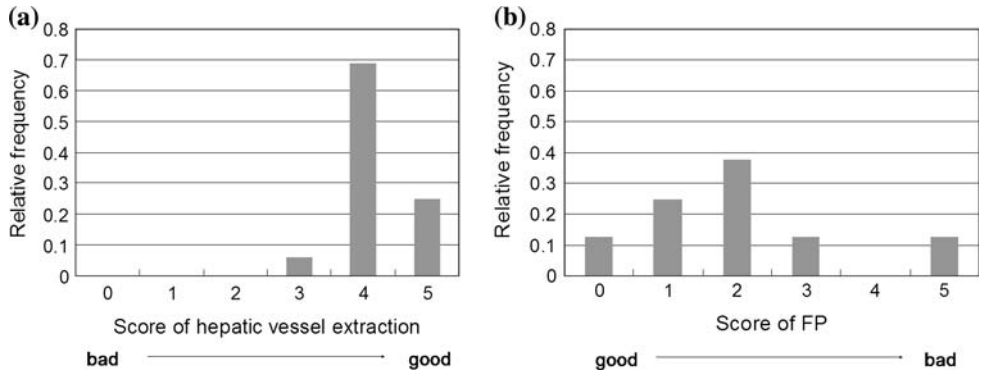

Fig. 8 Histograms of **a** hepatic-vessel extraction scores and **b** FP scores of our proposed hepatic-vessel extraction method evaluated by a radiologist. Hepatic-vessel extraction was scored within the range from 0 to 5 by a radiologist. If the vessel extraction score was close to 5 points, the result of vessel extraction meant that it was good. The number of FPs was also evaluated with scoring within the range from 0 to 5 by a radiologist. If the score of FP was close to 0, this meant that there were few FPs in the extraction results

Gaussian filter ($\sigma = 1.5$) is a practical solution that needs only 90 s to complete the smoothing process. The Gaussian filter was selected and used for smoothing in this study.

The histograms of the hepatic-vessel region and of the other liver-tissue regions are investigated after each processing step of our approach. Two values in the histogram (mean value and standard deviation of the contrast) are used for evaluating the separation ratio between the hepatic-vessel regions and the other liver regions in the images. The separation ratio S_{ab} between two distributions, *a* and *b*, is defined by the following equation:

$$S_{ab} = \frac{|\mu_a - \mu_b|}{\sqrt{(\sigma_a N_a + \sigma_b N_b)/(N_a + N_b)}}, \quad (7)$$

where N_a and N_b are the numbers of all samples of *a* and *b*, μ_a and μ_b are the mean values of *a* and *b*, and σ_a and σ_b are the standard deviations of *a* and *b*, respectively. If S_{ab} is close to 0, it means that *a* and *b* overlap and cannot be separated. Otherwise, a high value of S_{ab} indicates that overlap between *a* and *b* is small and a thresholding process can separate *a* and *b* easily. Figures 5 and 6 show the histograms obtained from the result of each processing step in our approach (the true vessel regions extracted by a radiologist were used for evaluations of the separation ratio). The results show that the separation ratio was increased from 5.8 to about 31 after smoothing and contrast enhancement. Although the multi-scale line filter caused a small decrease by a factor of about three in the separation ratio, it can reduce the FP regions (Fig. 2) of the hepatic vessels, which is very important for the segmentation process. Such results show that the basic consideration of this study (amplifying the difference in CT number between the hepatic-vessel regions and the other liver-tissue regions) is realized successfully.

The accuracy of the segmentation of the hepatic-vessel regions is very sensitive to the threshold value th_g given in Sect. 2.4. We varied the value of th_g and observed the true positive (TP) and FP ratios of the hepatic vessels during the segmentation process. First of all, the true vessel regions (gold standard) are determined by a radiologist. If the true vessel region and the hepatic-vessel-candidate region are overlapped, these overlapped regions are regarded as TPs. The other regions of the hepatic-vessel-candidate are regarded as FPs. Figure 7 shows the change in the accuracy of the segmentation represented by the relationship between the TP and FP ratios of the hepatic-vessel regions according to the different values of th_g. The results indicate that the total performance of the hepatic-vessel segmentation is not very high (TP ratio: 50% at FP ratio: 5% at $th_g = \mu$). We found TP ratio (the ratio of the hepatic-vessel

regions correctly extracted by the computer) was not suitable for evaluation of the accuracy of the line pattern extraction, some other evaluation methods should be introduced in the next stage. However, the fact that a simple thresholding process can extract the hepatic vessels from plain CT images represents progress, and such techniques can be expected to expand the use of plain CT images in the diagnosis of liver diseases.

The results of hepatic-vessel (hepatic veins and portal veins) extraction from plain CT images of 16 patients were evaluated by a radiologist. In the evaluation of hepatic-vein and portal-vein extraction, we use a protocol for visual evaluation with advices from a radiologist. The protocol of evaluation is as follows: First, the accuracy of hepatic-vessel extraction (the number of TPs) is judged and is scored within the range from 0 to 5 by a radiologist. If the judgment of vessel extraction scores close to 5 points, the result of vessel extraction is considered good. In the judgment of hepatic-vessel extraction, the extraction of anatomic vessel branches and the accuracy of the hepatic-vessel shape with consideration of anatomic structures are used. Second, the over extraction (the number of FPs) is evaluated with scoring within the range from 0 to 5 by a radiologist. If the score of FPs is close to 0, this means that there are few FPs in the extraction results.

Histograms of the mean and standard deviation of the TP and FP scores are shown in Fig. 8. The mean and standard deviation of the TP scores were about 4.19 and 0.50, respectively, and the mean and standard deviation of the FP scores were about 2.00 and 1.44, respectively. This result shows that the TP scores of hepatic-vessel extraction are high in all cases, but the FP scores of hepatic-vessel extraction are varied largely in different CT cases. We found that failures of hepatic-vessel extraction utilized by our method are caused by incomplete approximation of gray-scale-level distribution of hepatic vessels. A radiologist pointed out that extracted hepatic vessels are narrow in comparison with the original vessels in CT images. The same radiologist also pointed out that FPs of hepatic-vessel extraction are occurred in liver verge and S1 area of Couinard liver segments. Solutions of these problems will be sought in our future work.

5 Conclusion

We propose a fully automated approach to extraction of hepatic vessels including the portal vein and hepatic vein in plain X-ray CT images. The hepatic vessels in the liver region were enhanced by use of a Gaussian-based density transformation and selected by use of Hessian-based line filtering. The accuracy of the vessel extraction was evaluated based on a quatitative comparision between the plain CT images and contrast-enhanced CT images from the same patient and a visual observation by a radiologist who specialized in liver diagnosis. The preliminary results showed that even the density difference between hepatic vessels and other liver regions was very small in plain CT cases, and that the proposed method can enhance and identify most of the vessel regions as well as the human observer can. However, many FP regions occurred in the vessel identification process due to the noise in CT images; this has to be improved in future work with the use of additional data.

We confirmed that the performance of our automated hepatic-vessel identification algorithm is almost comparable to that of human observers. This result shows the potential for extraction of liver lobes and liver structures (useful for the diagnosis of cirrhosis) in plain CT images.

Acknowledgments The authors would like to thank Mr. T. Kitagawa, Dr. G. Lee, and other members of the Fujita Laboratory for their collaboration and comments. The authors also would like to thank a reviewer and an associated editor for their constructive suggestions for improving our manuscript. This research was partly supported by a Grant-in-Aid for Scientific Research on Priority Areas, and in part by the Ministry of Health, Labour, and Welfare under a Grant-In-Aid for Cancer Research, Japanese Government.

References

1. Kobatake H, Future CAD. in multi-dimensional medical images—project on multi-organ, multi-disease CAD system. Comput Med Imag Graph. 2007;31:258–66.
2. Doi K. Computer-aided diagnosis in medical imaging: historical review, current status and future potential. Comput Med Imaging Graph. 2007;31:198–211.
3. Nishikawa RM. Current status and future directions of computer-aided diagnosis in mammography. Comput Med Imaging Graph. 2007;31(4–5):224–35.
4. Baker JA, Lo JY, Delong DM, Floyd CE. Computer-aided detection in screening mammography: variability in cues. Radiology. 2004;233:411–7.
5. van Ginneken B, ter Romeny BM, Viergever MA. Computer-aided diagnosis in chest radiography: a survey. IEEE Trans Med Imaging. 2001;20:1228–41.
6. Li Q. Recent progress in computer-aided diagnosis of lung nodules on thin-section CT. Comput Med Imaging Graph. 2007;31(4–5):248–57.
7. Yoshida H, Nappi J. CAD in CT colonography without and with oral contrast agents: progress and challenges. Comput Med Imaging Graph. 2007;31(4–5):267–84.
8. Bogoni L, Cathier P, Dundar M, Jerebko A, Lakare S, Liang J, et al. Computer-aided detection (CAD) for CT colonography: a tool to address a growing need. Br J Radiol. 2005;78:S57–62.
9. Selle D, Preim B, Schenk A, Peitgen H-O. Analysis of vasculature for liver surgical planning. IEEE Trans Med Imaging. 2002;21:1344–57.
10. Frericks BB, Caldarone FC, Nashan B, Savellano DH, Stamm G, Kirchhoff TD, et al. 3D CT modeling of hepatic vessel architecture and volume calculation in living donated liver transplantation. Euro Radiol. 2004;14:326–33.

11. Hermoye L, Laamari-Azjal I, Cao Z, Annet L, Lerut J, Dawant BM, et al. Liver segmentation in living liver transplant donors: comparison of semiautomatic and manual methods. Radiology. 2005;234:171–8.
12. Zhang X, Kanematsu M, Fujita H, Hara T, Hoshi H. Computerized classification of liver disease in MRI using artificial neural network. Proc SPIE Med Imaging. 2001;4322:1735–42.
13. Park H, Bland PH, Meyer CR. Construction of an abdominal probabilistic atlas and its application in segmentation. IEEE Trans Med Imaging. 2003;22(4):483–92.
14. Sato Y, Okada T, Nakamoto M, Chen YW, Hori M, Sugano N, et al. Computational modeling of anatomical structures. In: Symposium on future CAD, proc. of the second international symposium on intelligent assistance in diagnosis of multi-dimensional medical images, 2006, p. 42–9.
15. Sato Y, Nakajima S, Shiraga N, Atsumi H, Yoshida S, Koller T, et al. Three-dimensional multi-scale line filter for segmentation and visualization of curvilinear structures in medical images. Med Image Anal. 1998;2:143–68.
16. Sato Y, Westin C-F, Bhalerao A, Nakajima S, Shiraga N, Tamura S, et al. Tissue classification based on 3D local intensity for volume rendering. IEEE Trans Vis Comput Graph. 2000;6:160–70.
17. Zhou X, Kitagawa T, Hara T, Fujita H, Yokoyama R, Kondo H, et al. Constructing a probabilistic model for automated liver region segmentation using non-contrast X-ray torso CT images. In: Proceedings of of 9th MICCAI, vol. 1; 2006, p. 856–63.
18. Kawajiri S, Zhou X, Zhang X, Hara T, Fujita H, Yokoyama R, et al. An automatic extraction method of liver vessels in non-contrast X-ray CT images (in Japanese). Med Imaging Inf Sci. 2007;23:141–4.